

The induced emf on the pickup coil due to the DHVA magnetization of frequency  $F_i$  is given by

$$\text{emf}_i = d/dt[\mathbf{M}_i(\mathbf{B}) \cdot \hat{\mu}] \simeq -\hat{\mu} \cdot \boldsymbol{\alpha}_i(\mathbf{B}_0) \sum_{n=1}^{\infty} [\sin(2\pi F_i/B_0 + \beta_i + \frac{1}{2}(n\pi))] J_n(X) 2n\omega \sin n\omega t, \quad (\text{A3})$$

where  $\hat{\mu}$  is a unit vector along the pickup coil axis and  $X$  is defined by

$$X = 2\pi F_i H_m / B_0^2.$$

## Specific-Heat Anomaly and Calculation of the Configurational Entropy Change at the Phase Transition in Copper Formate Tetrahydrate\*

KENKICHI OKADA

*Nagoya Institute of Technology, Gokiso-cho, Showa-ku, Nagoya, Japan*

(Received 4 May 1967)

Specific-heat anomalies of copper formate tetrahydrate,  $\text{Cu}(\text{HCOO})_2 \cdot 4\text{H}_2\text{O}$ , and its deuterium substitute  $\text{Cu}(\text{HCOO})_2 \cdot 4\text{D}_2\text{O}$  were found at respective antiferroelectric transition points. It has a typical  $\lambda$  shape, sharply peaked at the transition. The transition point was shifted from  $-37.7$  to  $-27.5^\circ\text{C}$  by deuterium substitution. The transition entropies were measured as 0.78 and 0.90 cal/mole deg in hydrated and deuterated crystals, respectively. The transition was considered to be due to an order-disorder phenomenon arising from the hydrogens in the water of crystallization. The number of configurations of hydrogens in the water layer of the structure, the positions of which have been determined by a previous neutron-diffraction study at room temperature, was calculated taking account of the full correlation through oxygens by the use of a simple equivalent model. A different value was obtained from that obtained by Pauling's method; the latter does not agree with experiment in this layer-structured crystal. The configurational entropy change between the disordered and the antiferroelectric states was calculated as  $R \ln \frac{1}{2}(2 + \sqrt{2}) \simeq 1.06$  cal/mole deg. The theoretical value agrees well with the experimental values obtained from thermal measurements on both crystals.

### I. INTRODUCTION

COPPER formate tetrahydrate,  $\text{Cu}(\text{HCOO})_2 \cdot 4\text{H}_2\text{O}$ , has been investigated extensively because of its magnetic properties at low temperatures. On the other hand, in 1962 Kiriya<sup>1</sup> reported a dielectric anomaly in this crystal at  $-36^\circ\text{C}$ , and a mechanism of the anomaly was proposed. The crystal structure, including copper, carbon, and oxygen positions, was determined by Kiriya *et al.*,<sup>2</sup> who found the crystal to be monoclinic, space group  $P2_1/a$  with  $a=8.18$ ,  $b=8.15$ ,  $c=6.35$  Å, and  $\beta=101^\circ 5'$ , and with two formula units per unit cell. A neutron-diffraction study<sup>3</sup> was performed in order to obtain the positions of the hydrogens in the water of crystallization at room temperature. During this study some hydrogens were found to be disordered. This stimulated us to measure dielectric properties in detail, and the dielectric anomaly mentioned above was

actually found to be due to an antiferroelectric phase transition.<sup>4</sup>

As determined by Kiriya *et al.*,<sup>2</sup> this crystal has a structure consisting of alternating layers of waters and copper formate groups in the (001) plane. Mookherji and Mathur<sup>5</sup> predicted a two-dimensional antiferromagnetism at low temperature, because of its layer structure. In a similar fashion, a two-dimensional ordering of hydrogens in the water layer which may correspond to the antiferroelectric phase can be expected. As a matter of fact, the neutron-diffraction study<sup>3</sup> showed that the disordered hydrogens are only in the water layer, while the hydrogens bonding water oxygens to formate oxygens are ordered at room temperature. It is plausible that the disordered hydrogens are ordered below the transition point. This order-disorder transition may give an excess entropy detectable by thermal measurements.

The configurational entropy of the order-disorder transition due to hydrogen may be calculated by

\* Work supported in part by a grant-in-aid for scientific research from the Ministry of Education, Japan.

<sup>1</sup> H. Kiriya, *Bull. Chem. Soc. Japan* **35**, 1199 (1962).

<sup>2</sup> R. Kiriya, H. Ibamoto, and K. Matsuo, *Acta Cryst.* **7**, 482 (1954).

<sup>3</sup> K. Okada, M. I. Kay, D. T. Cromer, and I. Almodovar, *J. Chem. Phys.* **44**, 1648 (1966).

<sup>4</sup> K. Okada, *Phys. Rev. Letters* **15**, 252 (1965).

<sup>5</sup> A. Mookherji and S. C. Mathur, *J. Phys. Chem. Solids* **24**, 1386 (1963).

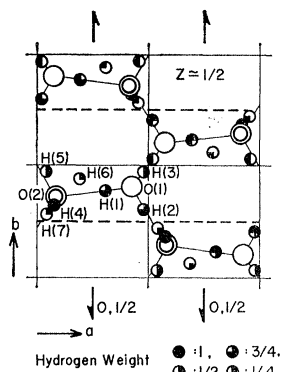


FIG. 1. Structure of the water layer at room temperature. Weights of disordered hydrogens are indicated.

Pauling's method. This has been carried out for ice<sup>6</sup> and a typical hydrogen-bonded ferroelectric crystal, potassium dihydrogen phosphate,<sup>7</sup> both of which gave good agreement with the experimental values. Figure 1 illustrates the structure of the water layer projected on the (001) plane. Oxygens O(1) and O(2) are non-equivalent. The probabilities of finding hydrogens at the respective positions in the disordered state are given in the figure by symbols. As in the case of ice, an oxygen should have two and only two hydrogens attached, and a hydrogen bond should contain one hydrogen between two oxygens. Since O(2) has a hydrogen H(4) with a probability of unity which bonds it to an oxygen in a formate group in the other kind of layer, we should add only one hydrogen close to it. We have six hydrogen bonds per molecule. There are  $2^{6N}$  configurations of hydrogen, many of which should be excluded by the above-mentioned restrictions, where  $N$  is the number of molecules. The reduction factor turns out, at once, to be  $\frac{3}{8}$  per oxygen for both kinds. Therefore, the number of configurations becomes  $2^{6N} (\frac{3}{8})^{4N} = (\frac{9}{8})^{2N}$ , which gives the configurational entropy  $2R \ln(\frac{9}{8}) \approx 0.47$  cal/mole deg. This value is too small when compared with experimental values presented here for both hydrated and dehydrated crystals, even though we have neglected the Boltzmann factor.

This discrepancy may be attributed to an insufficient consideration of the correlations through oxygens as pointed out by Meijering<sup>8</sup> in the case of ice. This effect is probably enhanced in the two-dimensional structure of this crystal. Slater's postulates in his theoretical treatment of potassium dihydrogen phosphate<sup>9</sup> are also inconclusive because of an insufficient consideration of the correlations. It is the purpose of this paper to report the experimental results of the specific-heat anomaly and to work out the calculation of the configurational entropy taking the full correlation through oxygen atoms into consideration and to compare it with the

<sup>6</sup> L. Pauling, *The Nature of the Chemical Bond* (Cornell University Press, Ithaca, New York, 1960).

<sup>7</sup> C. C. Stephenson and J. G. Hooley, *J. Am. Chem. Soc.* **66**, 1397 (1944).

<sup>8</sup> J. L. Meijering, *Disc. Faraday Soc.* **23**, 83 (1957).

<sup>9</sup> J. C. Slater, *J. Chem. Phys.* **9**, 16 (1941).

experimental value. The order-disorder phenomenon associated with hydrogens is confirmed.

## II. EXPERIMENTAL

Specific heats of both hydrated and dehydrated crystals,  $\text{Cu}(\text{HCOO})_2 \cdot 4\text{H}_2\text{O}$  and  $\text{Cu}(\text{HCOO})_2 \cdot 4\text{D}_2\text{O}$ , were measured by an adiabatic calorimeter over temperature ranges including their respective transition points. The adiabatic condition was obtained with a temperature-controlled alcohol bath that followed the temperature change of the specimen to an accuracy of  $\pm 5/1000^\circ\text{C}$ , using a differential thermocouple. Heat flows into powder specimens of 61.1 and 99.6 g from a small heater were 51 and 75 mW for the hydrated and dehydrated crystals, respectively.

The experimental values versus temperature were on a good straight line from  $-70$  to  $+40^\circ\text{C}$  except in the vicinity of the transition point. At  $+44.5^\circ\text{C}$ , the dehydration temperature of the hydrated crystal, a sharp increase of the specific heat appeared. Specific-heat anomalies near the transitions for both crystals are plotted in Fig. 2. They showed  $\lambda$ -shaped anomalies at their respective transition temperatures. The transition point was shifted to higher temperature by about  $10^\circ\text{C}$  by deuterium substitution in the water of crystallization. It may show that the transition is closely related to hydrogens in the water. Integrating the heat flow-in above the base line, the transition enthalpy was obtained. The transition entropy was also integrated. These thermal parameters<sup>10</sup> are tabulated in Table I. Seki *et al.*<sup>11</sup> measured the specific heat of a hydrated crystal from  $2^\circ\text{K}$  up to room temperature. Their value is also cited in the table.

The values of transition entropy are quite reasonable for an order-disorder transition. These values will be

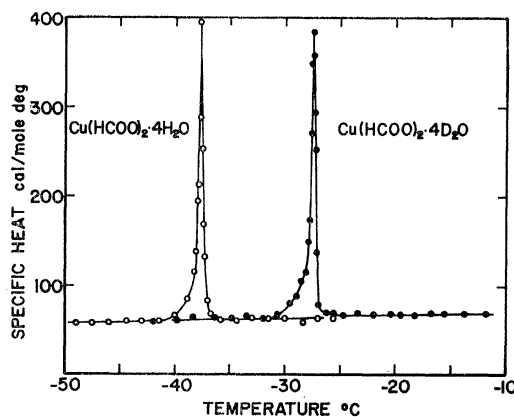


FIG. 2. Specific-heat anomalies at the transitions.

<sup>10</sup> In previous publications (Refs. 3 and 4), the transition point of hydrated crystal was reported as  $-38.9^\circ\text{C}$ . The present examinations revealed that the earlier data contained a large error in the temperature measurement.

<sup>11</sup> S. Seki and H. Suga (private communication).

compared with a theoretical value calculated below using a simple model.

### III. EQUIVALENT MODEL FOR CALCULATION OF THE ENTROPY

The two-dimensional hydrogen bond network in the water layer is shown schematically in Fig. 3. Remembering the two restrictions on configuration of hydrogen atoms and the fact that oxygen O(2) had only one disordered hydrogen, we see easily that an O(2)-O(2) pair has four possible hydrogen configurations as shown in Fig. 4(a), in which the ordered hydrogen H(4) is omitted. Now we consider an O(1)-O(1) pair, all of whose hydrogens are disordered. This pair connects four O(2)-O(2) pairs as shown in Figure 4(b). When one of the O(2)-O(2) pairs—the bottom pair in the figure, for example—has a hydrogen toward the central O(1)-O(1) pair, the hydrogen configuration in the O(1)-O(1) pair will be as shown. Other O(2)-O(2)

TABLE I. Thermal parameters of the transition.

	Transition point (°C)	Enthalpy $\Delta H$ (cal/mole)	Entropy $\Delta S$ (cal/mole deg)
Cu(HCOO) <sub>2</sub> 4H <sub>2</sub> O	-37.7	185	0.78
Cu(HCOO) <sub>2</sub> 4H <sub>2</sub> O <sup>a</sup>	-37.2	200	0.85
Cu(HCOO) <sub>2</sub> 4D <sub>2</sub> O	-27.5	221	0.90
Cu(DCOO) <sub>2</sub> 4D <sub>2</sub> O <sup>b</sup>	-27.1	...	...

<sup>a</sup> Reference 11.

<sup>b</sup> Reference 13.

pairs can not have any hydrogens toward the O(1)-O(1) pair at all. In other words, one O(2)-O(2) pair out of four presents one hydrogen atom to the O(1)-O(1) pair, and the configuration for the O(1)-O(1) pair is uniquely determined. This configuration occurs with a probability of  $\frac{1}{4}$ . Considering this and four configurations in the O(2)-O(2) pair, the hydrogen weights as shown in Fig. 1, the result of the neutron diffraction,<sup>3</sup> are obtained.

Taking account of this, O(2)-O(2) pairs can, for simplicity, be symbolized by arrows which correspond to the actual hydrogen configurations as illustrated in Fig. 4(a). An arrow can point in four possible directions. Hydrogens in the O(1)-O(1) pair need not be considered, since their positions are determined uniquely by hydrogens in four O(2)-O(2) pairs, for example, as shown in Fig. 4(b). More than one arrow can not point toward the O(1)-O(1) pair, because it will violate the restriction on the hydrogen bond. Using this symbol, an equivalent model, considering only hydrogen configuration, will be a square net, each unit cell of which has an arrow pointing to one of four corners. This net

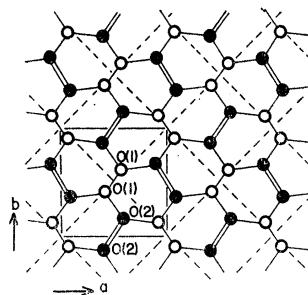


FIG. 3. Hydrogen-bond network in the water layer. Dotted lines show the square net of the model used for the calculation.

is shown in Fig. 5 and by dotted lines in Fig. 3. The cell in the net corresponds to one-half of the unit cell of the crystal lattice, and it contains one O(1)-O(1) and one O(2)-O(2) pair.

In this two-dimensional square array of arrows, an arrow can point to one of four corner points surrounding it, but more than one adjacent arrow can not point to a given corner point at the same time. Now our problem is to count the number of ways to place arrows which are not mutually independent of each other under the above-mentioned restriction in the square net. The number of cells is the number of molecules of the crystal. Every point must have one of four surrounding arrows pointing to it. This means that no vacancy is allowed except at edges, as shown in Fig. 5, if we put a small solid circle at the corner point to which an arrow points.

### IV. ONE-DIMENSIONAL CHECKERBOARD

First, we consider a one-dimensional array of arrows—a one-dimensional checkerboard—as shown in Fig. 6. This checkerboard has  $n$  arrows in  $n$  cells with  $2(n+1)$  corner points. Let the number of configurations of this one-dimensional model be  $P(n)$ . The  $P(n)$  is divided into two terms as

$$P(n) = A(n) + B(n). \quad (1)$$

Here,  $A(n)$  is the number of configurations when the last arrow in the right-end cell points to one of the two last corner points, i.e., toward the right, as shown in

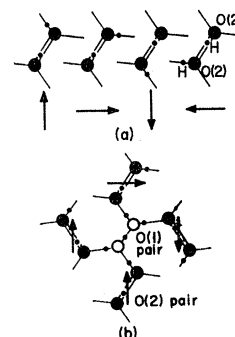


FIG. 4. (a) Four possible hydrogen configurations in an O(2)-O(2) pair. (b) Hydrogen configuration in an O(1)-O(1) pair uniquely determined by four O(2)-O(2) pairs. Ordered hydrogens are omitted. Arrows symbolize different configurations.

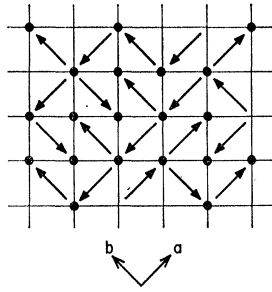


FIG. 5. Two-dimensional checkerboard showing the equivalent model used in the calculation. A small solid circle at a corner-point shows that it is pointed to by an arrow.

Fig. 6(a), and  $B(n)$  is that number when the last arrow points to one of the two next-to-last corner points. That is, the last two points are vacant as in Fig. 6(b). These two cases are mutually exclusive; thus, Eq. (1) holds.

For the case of  $n+1$ ,

$$P(n+1) = A(n+1) + B(n+1). \tag{2}$$

The first term  $A(n+1)$  in Eq. (2) is evidently two times  $P(n)$ , since the addition of a new cell having an arrow toward the right implies no restriction on the previous configuration with  $n$  arrows, i.e., the last cell may be added to either (a) or (b), and the last arrow has two possibilities in this case [see Fig. 6(c)]. When the arrow in the new cell points left, the next-to-last arrow has three possibilities. In the case of Fig. 6(d), we have  $B(n) + A(n)/2$  configurations, in which the first term stands for cases when the next-to-last arrow points to its two left corner points and the second term represents the case when it points right toward the corner point unoccupied by the last arrow. Since the last arrow has two possibilities, it is multiplied by 2. Now we have the relations

$$A(n+1) = 2A(n) + 2B(n)$$

and

$$B(n+1) = A(n) + 2B(n).$$

From these, we easily obtain

$$2A(n-1) - 4A(n) + A(n+1) = 0,$$

and exactly the same equation for  $B$ . Adding two equations for  $A$  and  $B$ , from Eq. (1), we have a linear difference equation to be solved as follows:

$$2P(n-1) - 4P(n) + P(n+1) = 0. \tag{3}$$

The general solution of this difference equation is

$$P(n) = 2^{n/2}(C_1 e^{n\phi} + C_2 e^{-n\phi}), \tag{4}$$

where  $\cosh \phi = 2$ . We have boundary conditions

$$P(1) = 4 \quad \text{and} \quad P(2) = 14,$$

which correspond to numbers of configurations for one cell and two cells, respectively. With these boundary

conditions, from Eq. (4), the solution of Eq. (3) turns out to be

$$P(n) = 2^{n/2} [e^{\phi(n-1)} (\frac{7}{2} - \sqrt{2}e^{-\phi}) + e^{-\phi(n-1)} (\sqrt{2}e^{\phi} - \frac{7}{2})].$$

Neglecting the second term in the square brackets for large  $n$ , and using  $\exp \phi = \sqrt{2} + 1$ , we have

$$P(n) = (2 + \sqrt{2})^n (1 + \sqrt{2}) / 2.$$

Taking the logarithms of both sides of this equation, we can neglect the term  $\ln(1 + \sqrt{2}) / 2$  for large  $n$ . The logarithm of the number of configurations of the one-dimensional checkerboard is, for large  $n$ ,

$$\ln P(n) = n \ln(2 + \sqrt{2}). \tag{5}$$

### V. TWO-DIMENSIONAL CHECKERBOARD

The second step is to build up a two-dimensional checkerboard stacking one-dimensional checkerboards obtained in the preceding section. In a one-dimensional checkerboard, if it is long enough and the effect of ends is neglected, the probability of finding a point at the head of an arrow, i.e., of having a solid circle at a point as seen in the figures, can be considered as  $\frac{1}{2}$ , since we have  $n$  arrows and  $2(n+1)$  points. We may select two one-dimensional checkerboards out of  $P(n)$  which fit together at all points, making a two-lined checkerboard as shown in Fig. 7. In the two-lined checkerboard, the probability of finding a point at the head of an arrow is seen to be unity for an inside point and  $\frac{1}{2}$  for a point on the edge. The same is true for an  $m$ -lined checkerboard built up by successive stackings. Therefore, the fitting probability for one pair of points is  $(\frac{1}{2})^2 + (\frac{1}{2})^2$ , that is, the sum of the probability of occupancy of the upper point of the pair times that of the vacancy of the lower point and vice versa. Then, the fitting probability of two checkerboards as a whole is  $(\frac{1}{2})^n$ , independent of the number of lines.

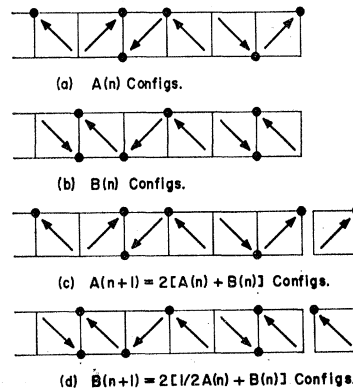


FIG. 6. Building up of the one-dimensional checkerboard cell by cell.

Calling the number of configurations of a checkerboard with  $n$  rows and  $m$  lines  $Q(n, m)$ , we obtain in general

$$Q(n, i) = Q(n, i-1)Q(n, 1)\left(\frac{1}{2}\right)^n,$$

from which, taking logarithms,

$$\ln Q(n, m) = m \ln Q(n, 1) + n(m-1) \ln \frac{1}{2}.$$

In this equation, from Eq. (5),

$$\ln Q(n, 1) = \ln P(n) = n \ln(2 + \sqrt{2}).$$

For large  $m$ ,

$$\ln Q(n, m) = nm \ln(2 + \sqrt{2})/2.$$

This is the number of configurations of a two-dimensional checkerboard for which we are looking. In the calculation, no vacancy is allowed except at edges of the board. Since the number of cells is equal to the number of molecules in the crystal  $N$ , we can put  $nm = N$ . Multiplying by the Boltzmann constant  $k$ , the configurational entropy of the disordered state is given by

$$\begin{aligned} k \ln Q(n, m) &= kN \ln(2 + \sqrt{2})/2 \\ &= R \ln(2 + \sqrt{2})/2, \end{aligned} \quad (6)$$

where  $R$  is the gas constant. Actually, two-dimensional checkerboards themselves are stacked to form a three-dimensional crystal. When the crystal is large enough and the edge effect is neglected, however, no modification is necessary.

## VI. COMPARISON WITH THE EXPERIMENTS AND DISCUSSIONS

The structure analysis by neutron diffraction below the transition is not complete at this time. By inspection of the results of the dielectric<sup>3,4</sup> and thermal studies of the crystal, however, ordering or at least two-

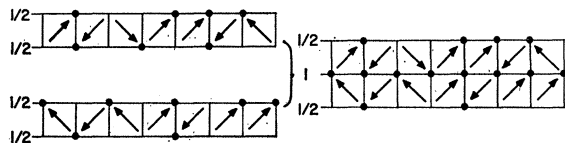


FIG. 7. Stacking of two one-dimensional checkerboards. The number on a line indicates the probability of finding a point on that line at the head of an arrow.

dimensional ordering<sup>12</sup> of the hydrogens can be expected below the transition point. The configurational contribution to the entropy below the transition point may be neglected. Therefore, we obtain the configurational transition entropy change from Eq. (6) as

$$\Delta S = R \ln(2 + \sqrt{2})/2 \simeq 1.06 \text{ cal/mole deg.}$$

The theoretical value and the experimental values, summarized in Table I, of the transition entropy agree fairly well. The small discrepancies may be attributed to two facts. We neglected statistical Boltzmann factors in the partition function; that is, we assumed that all of the four configurations of the O(2)-O(2) pair were energetically equivalent. Without neglecting this factor, we might obtain a smaller theoretical value. Second, disorder and order near the transition are by no means perfect. Therefore, we might have dropped some part of enthalpy spread over a rather wide temperature range.

The new calculation of the number of hydrogen configurations in the disordered state was successful in the layer-structured copper formate tetrahydrate. This method may be applied to other disordered structures if a simple equivalent model can be constructed.

Using this model, the ordered structure of the hydrogens below the transition might be predicted and the value of the polarization might be estimated. One of the possible structures which gives an antiparallel polarization along the  $b$  axis, the antiferroelectric axis, agrees well with the result of the NMR study by Soda *et al.*<sup>13</sup> Further discussion will be left until the neutron-diffraction study at low temperatures is complete.

## ACKNOWLEDGMENTS

The author wishes to express his appreciation to Professor Y. Takagi, Nagoya University, and Dr. M. I. Kay, Puerto Rico Nuclear Center, for their stimulating discussions. He is also indebted to Professor S. Seki and Dr. G. Soda, Osaka University, for communication of their unpublished data and for discussions, and to Dr. T. Ono of this Institute for valuable suggestions.

<sup>12</sup> A brief check by neutron diffraction below the transition showed that the space group  $P2_1/a$  is unchanged and the center of symmetry is kept. No superstructure line was found. From the result, we can imagine that ordering is only in the water layer and it is disordered along the  $c$ -axis direction. The center of symmetry is considered to be found by averaging over random stackings of two-dimensionally ordered sheets.

<sup>13</sup> G. Soda (private communication).